PHOTOELECTROCHEMICAL ELECTRON SPIN RESONANCE:- THE REDUCTION OF FLUORESCEIN AT ILLUMINATED MERCURY ELECTRODES

R.G. Compton, R.G. Harland, M.B.G. Pilkington, G.M. Stearn, P.R. Unwin and A.M. Waller

Physical Chemistry Laboratory, South Parks Road, Oxford OX1 3QZ, England.

INTRODUCTION

The work described here is concerned with the elucidation of the mechanism of the reduction of the dye fluorescein, in aqueous solution, when this is carried out at mercury electrodes illuminated with 390 nm. radiation. In particular in-situ electrochemical ESR is used to provide mechanistic information and to demonstrate the intermediacy of the semi-fluorescein radical anion. The work described utilises an apparatus described previously and shown to be suitable for such studies [1]. This is built around a channel electrode cell fabricated in silica which can be located within an ESR cavity without damaging the sensitivity of the latter, permitting the identification of radicals formed during photoelectrochemical reactions. Moreover the known pattern of flow in the channel cell enables the calculation of the concentration profiles of electrogenerated radicals and in this way the steady-state ESR signal (S) can be related to the electrode generating current (I), the solution flow rate (V/cm^3s^{-1}) and the electrode geometry [2-6].

Portugaliæ Electrochimica Acta, 5 (1987) 271-279

RESULTS AND DISCUSSION

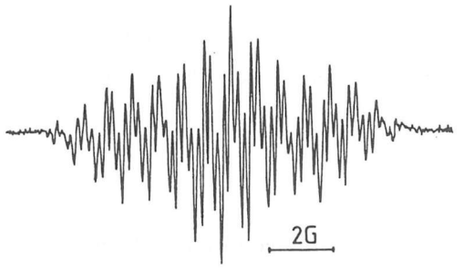

Figure 1. ESR spectrum attributed to the semi-fluorescein radical

We consider first the reduction of fluorescein at high pH (0.1 M NaOH). This was carried out at a mercury-coated copper foil channel electrode. Analysis of the recorded current voltage curves were consistent with a one-electron reversible reduction (E^o=1.19 V vs saturated calomel) as evidenced by Tafel analysis (which gave a slope of 59mV/decade) and Levich analysis [7] (which gave a diffusion coefficient of $3.2\times10^{-6}cm^2s^{-1}$, consistent with the literature value [8], by assuming a one-electron process). In-situ electrochemical ESR measurements carried out at potentials corresponding to the reduction wave revealed strong ESR signals attributable to the semi-fluorescein radical (S•) - see Figure 1 - confirming the dark reduction process to be

$$F + e^- = S^\bullet \qquad (a)$$

where

F = 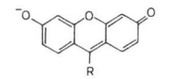

and

S• = 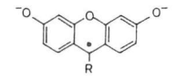

—R = 

The stability of S• under these conditions was established from the ESR signal - current - flow rate behaviour. We have previously shown [1] that for a stable radical

$$S = \text{constant}.I.V^{-2/3} \qquad (1)$$

Figure 2 shows a log-log plot of (S/I) vs V and the line drawn through the experimental points has the slope of ($^-$2/3) required by equation (1). Also shown in Figure 2 is the corresponding behaviour when the electrode is illuminated with 390 nm radiation. The loss of ESR signal intensity, particularly at low flow rates, is indicative of a photochemically induced decomposition of S•.

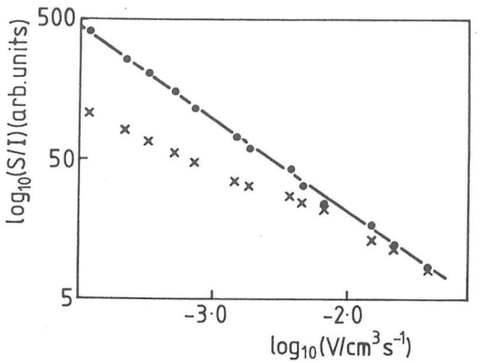

Figure 2. Variation of S/I with flow rate for S• radicals in the dark (0) and under illumination with 390 nm light (x).

Irradiation also induced significant photocurrents to flow - up to a maximum of twice the dark current under conditions of low flow rate and high light intensity. This suggested that the following reaction, involving an overall two electron transfer, was taking place;

$$H^+ + S\bullet + S\bullet^* \longrightarrow F + LH \qquad (b)$$

where

LH = 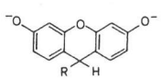

and $S\bullet^*$ denotes excited semi-fluorescein and LH is leucofluorescein. It is possible to conceive of reaction (b) occurring via one of several mechanisms. These are listed in Table 1. By analogy with the well known dark electrode reaction mechanisms [9,10] we identify "photo-DISP1" and "photo-DISP2" as conceivable mechanisms. Within the second category two possiblities - A and B - present themselves.

TABLE 1

"photo-DISP1"

$$F + e^- = S\bullet$$

$$S\bullet + h\nu = S\bullet^*$$

$$S\bullet^* + H^+ \xrightarrow[k_r]{\text{slow}} SH\bullet$$

$$\bullet^+ + S\bullet \xrightarrow{\text{fast}} F + LH$$

"photo-DISP2"

(A)

$$F + e^- = S\bullet$$

$$S\bullet + h\nu = S\bullet^*$$

$$S\bullet + S\bullet^* \xrightarrow[k_r]{\text{slow}} F^{2-} + F$$

$$F^{2-} + H^+ \xrightarrow{\text{fast}} LH$$

(B)

$$F + e^- = S\bullet$$

$$S\bullet + h\nu = SH\bullet^*$$

$$S\bullet^* + H^+ = SH\bullet^+$$

$$SH\bullet^+ + S\bullet \xrightarrow[k_r]{\text{slow}} F + LH$$

In the case of present interest the photo-DISP2(B) mechanism - which involves a protonation before the rate determining step - was rapidly eliminated since the photocurrents displayed no pH dependence within the (approximate) range 12.4 - 13.0. The two remaining possibilities were distinguished by calculating the photocurrent - flow rate behaviour through evaluating the 'effective' number of electrons transferred (N_{eff}: $1 < N_{eff} < 2$) in terms of the appropriate normalised rate constant K1 or K2 where

$$\text{photo-DISP1} \quad K1 = \frac{2I\epsilon}{\dfrac{1 + k_f}{k_r[H^+]}} \left[h^2 x_e^{\,2} / 9\bar{U}^2 D\right]^{1/3} \qquad (2)$$

$$\text{photo-DISP2} \quad K2 = \frac{2I\epsilon k_r[F]}{k_f} \left[h^2 x e^2 / 9\bar{U}^2 D\right]^{1/3} \qquad (3)$$

where D is the diffusion coefficient of F, I is the intensity of incident light (assumed to be constant across the cell depth), ϵ is the extinction coefficient of $S\bullet$, k_r represents the first-order rate constant for the decay of $S\bullet^*$ in the absence of chemical reaction, h is the half-height of the channel [1], $\bar{U}$ (cms^{-1}) is the mean solution velocity in the channel and x_e the electrode length. The two 'working curves' are shown in Figure 3. The calculation of these working

curves required the solution of the relevant coupled convective-diffusion equations and this was done numerically using the Backwards Implicit Method [11].

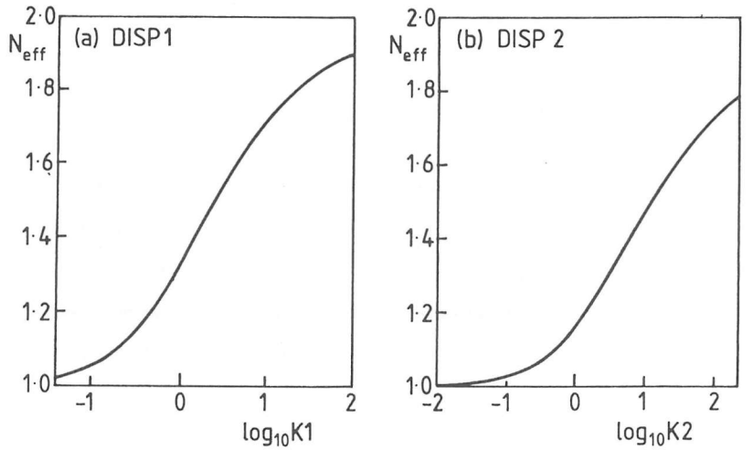

Figure 3. Working curves showing the effective number of electrons transferred as a function of the appropriate normalised rate constant for (a) 'photo-'DISP1'', and (b) 'photo-DISP2 (A)' processes.

Analysis of the experimental photocurrent - flow rate data in terms of the two mechanisms produced Figure 4 in which K1 or K2, as appropriate and as deduced via Figure 3, is plotted against $V^{-2/3}$. For both mechanisms acceptable straight lines are generated. However the two cases give rise to differing values of the kinetic terms in eqns (2) and (3): photo-DISP1:

$$\frac{2I\epsilon}{1 + \frac{k_r}{k_f[H^+]}} = 0.18s^{-1}$$

photo-DISP2(A):

$$\frac{2I\epsilon k_{r[F]}}{k_f} = 2.4 \pm 0.6 \times 10^5 mol^{-1}cm^3s^{-1}.$$

This was employed to achieve the sought mechanistic discrimination by applying the Backwards Implicit Method [11] to generate the S/I/V behaviour for the two mechanisms using the appropriate value of k_r/k_f for each as deduced from the photocurrent data. The theoretical results are compared with experiment in Figure 5. It is clear that satisfactory agreement is only found for the photo-DISP2(A) mechanism which we thus suggest to be the reduction pathway of fluorescein at irradiated mercury electrodes. Interestingly this is in contrast to the behaviour observed in the dark at more acidic pHs (9-10) where a DISP1 pathway operates as evidenced by chronoamperometry [12] and the half-wave potential/rotation speed dependence [13].

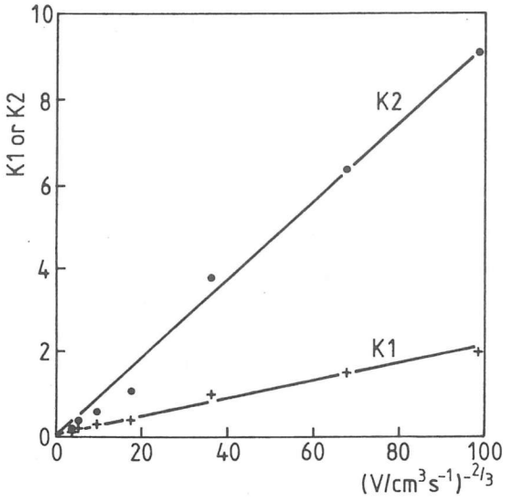

Figure 4. The dependence of K1 and K2 on the solution flow rate.

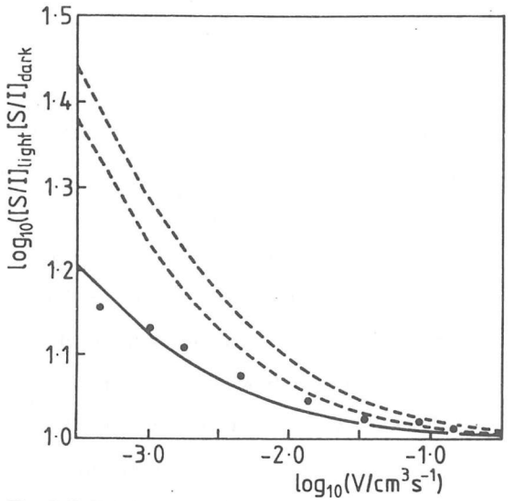

Figure 5. The S/I/V behaviour found experimentally (0) and as deduced from the photocurrent data assuming either a 'photo-DISP2(A)' (_____) or a 'photo-DISP1' (- -)process.

CONCLUSIONS

The reduction of fluorescein at illuminated mercury electrodes may be deduced as proceeding via a "photo-DISP2" pathway by means of of combined ESR and photoelectrochemical measurements. On the basis of the latter type of experiment in isolation unambiguous mechanistic assignment is not possible. The merits of combined electrochemical and spectroscopic techniques are again evident [14].

REFERENCES

1. B.A. Coles and R.G. Compton, J. Electroanal. Chem., 144, (1983),

2. R.G. Compton, D.J. Page and G.R. Sealy, J. Electroanal. Chem., 161, (1984), 129
3. R.G. Compton, D.J. Page and G.R. Sealy, J. Electroanal. Chem., 163, (1984), 65
4. R.G. Compton, P.J. Daly, P.R. Unwin and A.M. Waller, J. Electroanal. Chem., 191, (1985), 15
5. R.G. Compton, B.A. Coles and M.J. Day, J. Electroanal. Chem., 200, (1986), 205
6. R.G. Compton, B.A. Coles and M.J. Day, J. Chem Research, (1986), 260
7. R.G. Compton, and P.R. Unwin, J. Electroanal. Chem., 205, (1986)
8. P.J. Daly, D.J. Page and R.G. Compton, Anal. Chem., 55, (1983), 1191
9. C. Amatore, M. Gareil and J.M. Saveant, J. Electroanal. Chem., 147, (1983), 1
10. C. Amatore and J.M. Saveant, J. Electroanal. Chem., 85, (1977), 27
11. R.G. Compton, M.B.G. Pilkington and G.M. Stearn, JCS Faraday 1, in the press.
12. R.G. Compton, D. Mason and P.R. Unwin, JCS Faraday 1, in the press
13. R.G. Compton, R.G. Harland, P.R. Unwin and A.M. Waller, JCS Faraday 1, 83, (1987), 1261
14. R.G. Compton, and A.R. Hillman, Chem. Brit., 22, (1986) 1088